

Mechanical, Morphological and Chemical properties of Bio-degradable Nanocomposite Poly- Lactic acid/Mgo

Ku. Kanchan Arvind Ingle, Prof.Dr.G.S.Zamre, Prof. Dr.P.V.Thorat,
Department of Chemical Engineering, College of Engineering & Technology, Akola, Maharashtra, India

ABSTRACT

Incorporating small amounts of rigid nanoparticles within a polymer host to prepare polymer nanocomposites has shown great potential to enhance the physical, thermomechanical, and processing characteristics of pristine polymers since the 1990s. In this study, we first prepared Nanocomposite of PLA/MgO by *in situ* melt polycondensation. The morphological, mechanical, and thermal properties of PLA/MgO nanocomposites were characterized.

Key words:- Poly Lactic Acid, Nanocomposite, Morphology, Thermal Properties.

Date of Submission: 10-06-2021

Date of Acceptance: 24-06-2021

I. INTRODUCTION

Poly(lactic acid) (PLA) is a biodegradable and compostable polymer made from renewable resources; therefore, PLA nanocomposites have attracted intensive studies over the past decade. PLA nanocomposites exhibit enhanced physical (e.g., barrier, erosion resistance, and reduced flammability), thermomechanical (e.g., heat distortion temperature, thermal expansion coefficient, and stiffness), and processing (e.g., surface finish and melt strength) characteristics compared with pristine polymers. The work is on PLA nanocomposites with magnesium oxide (MgO) nanoparticles, and have been commercialized. Compared with commercial MgO, these nanoparticles have a much smaller crystal size, higher surface area, more surface defects, and higher reactivity. We have prepared PLA nanocomposites with MgO nanocrystals. At a MgO loading ratio of 0.4 wt% or less, mechanical properties of nanocomposites were significantly improved, probably because of the affinity PLA segments have for the MgO surface by bonding. However, because inorganic nanoparticles typically agglomerate and are not always miscible with the organic polymer phase, it is usually a challenge to achieve better dispersion and strong interfacial interaction between nanoparticles and the polymer matrix. One strategy to overcome this difficulty is to shield the particle with the same chains as the matrix polymer.

Our goal for the study is to prepare PLA nanocomposites with MgO nanoparticles through thermal compounding and compression molding. We hypothesized that MgO with PLA chains would

improve nanoparticle dispersion and yield nanocomposites with enhanced interfacial interaction due to chain entanglement and mechanical interlocking between the polymer matrix and PLA chains (Figure 1).

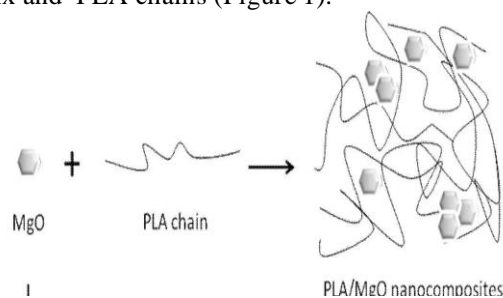
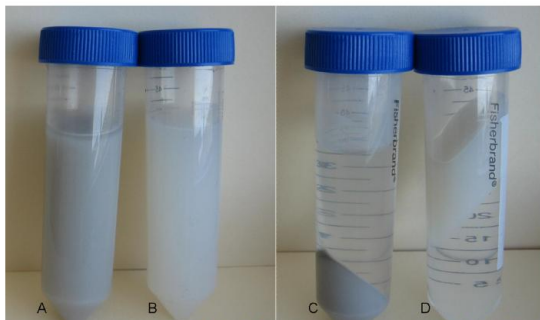


Figure 1 Schematic illustration of PLA/MgO nanocomposites.

II. EXPERIMENTAL SECTION

Preparation of PLA/MgO Nanocomposites

The PLA were ground through a 2 mm screen in a laboratory mill. Ground PLA, MgO, were dried in a vacuum oven at 80 °C for 24 h. Ground PLA with various amounts of MgO and (0.0125%, 0.025%, 0.05%, 0.2%, and 0.8%) were first mixed in a stand mixer for 10 min and then thermal compounded at 180 °C and 130 rpm for 5 min in an intensive mixer. After they cooled, the blends were ground into 2 mm powder. Pure PLA was treated with the same procedures used for the control. At least five specimens were prepared for each type of nanocomposite.



NANOCOMPOSITE SYNTHESIS



Fig. pouring of gel



Fig: -film before curing



Fig:-dry PLA film

III. RESULTS AND DISCUSSION

Mechanical Properties

Both PLA and its nanocomposites showed brittle fracture behavior, with 5.3 to 6.3% elongation at break. PLA exhibited tensile strength (σ) of 64 MPa and Young's modulus (E) of 1.6 GPa (Figure 2). With the addition of 0.0125% MgO, σ

and E were increased by 14% and 26%, respectively, compared with the values of PLA. The reinforcement of mechanical strength was probably caused by hydrogen bonding between ester groups in PLA chains and groups from the MgO. As the loading ratio of MgO further increased, σ and E decreased gradually but remained higher than the values of PLA. With 0.8% MgO, σ further decreased to 62 MPa.

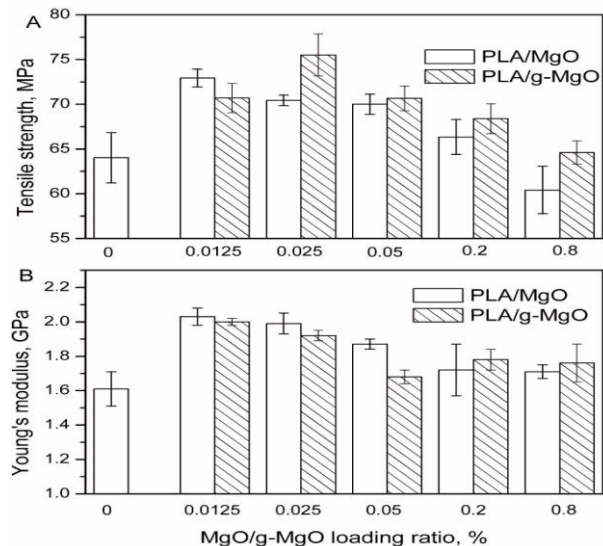


Figure 2 Tensile strength and Young's modulus of PLA/MgO nanocomposites.

For PLA/MgO nanocomposites, the maximum σ was observed with 0.025% MgO, and this value was 18% higher than the σ of PLA. Further increasing the MgO loading ratio to 0.05%, 0.2%, and 0.8% led to an obvious reduction in σ and a slight reduction in E . The σ of PLA/MgO nanocomposites was always slightly higher or similar to that of PLA/MgO nanocomposites, except for PLA/0.0125% MgO. The slight improvement in σ of the PLA/MgO nanocomposites could be a result of the enhanced penetration and interaction between the MgO nanoparticles and PLA matrix that occurred because of MgO nanocrystals. However, when the loading ratios of MgO increased beyond the optimal value, the agglomeration of nanoparticles became dominant and suppressed the interfacial interaction effect. Those agglomerations acted as local stress concentrations during the tensile test, and the mechanical strength consequently decreased. Moreover, because of the large number of groups from MgO nanoparticles, hydrolysis effects became obvious at higher concentrations of fillers, which also led to the deterioration of mechanical strength.

Morphology

The morphological changes of MgO are shown in Figure 3. MgO crystals existed in compact agglomerate forms with an average size of 10 to 15 μm . After which PLA chains, MgO exhibited a loose and porous morphology, indicating that the compact aggregation of the original MgO crystals was greatly inhibited.

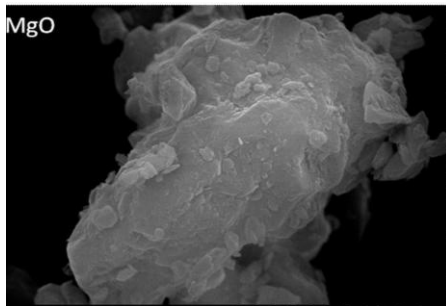


Figure 3 SEM images of MgO

An examination of the fracture surface of PLA/MgO nanocomposites (e.g., at 0.025%) revealed an obvious difference in the interfacial interaction between the polymer matrix and the nanofiller in these two systems. Most MgO nanoparticles (Figure 4), indicating a weak interfacial adhesion, MgO with PLA chains likely results in enhanced chain entanglement and mechanical interlocking with the polymer matrix and, consequently, better adhesion.

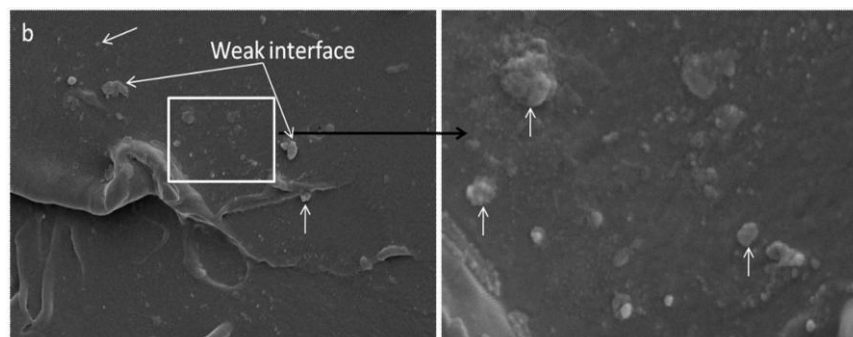


Figure 4 SEM images of PLA/MgO nanocomposites (nanoparticles are indicated with white arrows; right image is the squared section from left images with magnification).

Thermal Properties

Figure 5 shows DSC thermograms of PLA/MgO (A, first scan; C, second scan) DSC results are summarized in Table 1. The T_m and ΔH_m were obtained from the first heating scan to reveal the crystalline status of the molded nanocomposites; the T_g and ΔC_p were obtained from the second heating scan to erase the physical aging effect during storage. PLA/MgO nanocomposites

showed similar glass transition temperatures of about 59 $^{\circ}\text{C}$, and their heat capacity during glass transition [ΔC_p of 0.52 to 0.54 $\text{J}/(\text{g}\cdot^{\circ}\text{C})$] was similar to that of pure PLA, indicating that no strong chemical interactions were formed between the PLA matrix and nanoparticles. The melting temperature was also similar for all samples (148 to 149 $^{\circ}\text{C}$). The crystallinity of PLA was not obviously affected by addition of MgO.

Table 1 DSC results of PLA/MgO and PLA/MgO nanocomposites with various nanoparticle loading levels

MgO Sample	Mgo ratio (wt%)	T_g	ΔC_p	T_m	ΔH_m	X_m
		$^{\circ}\text{C}$	$\text{J}/(\text{g}\cdot^{\circ}\text{C})$	$^{\circ}\text{C}$	J/g	%
PLA	0	59.4	0.53	149.4	22.2	23.7
PLA/MgO	0.0125	58.9	0.53	148.4	21.1	22.5
	0.025	59.0	0.54	148.9	19.7	21.0
	0.05	59.1	0.52	147.6	23.6	25.2
	0.2	59.1	0.53	148.4	21.7	23.2
	0.8	59.4	0.54	148.6	21.9	23.4

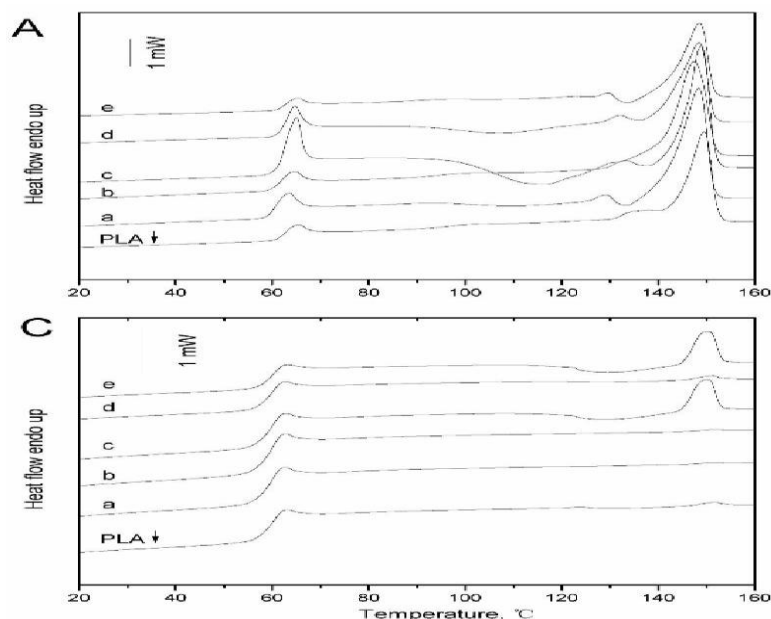


Figure 5 DSC thermograms of PLA/MgO (A, first scan; C, second scan) nanocomposites with various nanoparticle loading levels (a, 0.0125%; b, 0.025%; c, 0.05%; d, 0.2%; e, 0.8%).

TGA and derivative TGA thermograms of PLA/MgO nanocomposites are shown in Figures 6. Compared with the TGA thermogram curves of pure PLA, those of PLA/MgO nanocomposites shifted toward lower temperatures. As MgO loading ratio increased, the onset decomposition temperature, peak decomposition temperature (T_{max}), and end decomposition temperature decreased (Figure 6B). At 0.8% MgO, T_{max} was reduced by 48 °C compared with that of pure PLA.

In PLA/MgO nanocomposites, many surface hydroxyl groups from MgO were still available; therefore, decreased thermal stability was observed for all samples.

REFERENCES

- [1]. Benabdillah, K. M., Boustta M., Coudane J., & Vert M. (2001). Chap. 14 Can the Glass Transition Temperature of PLA Polymers Be Increased? In *Polymers from Renewable Resources: Biopolyesters and Biocatalysis*, ed. by Carmen Scholz, Richard A. Gross, ACS publication, pp 200-220.
- [2]. Bezrodna, T., Puchkovska, G., Shimanovska, V., Chashechnikova, I., Khalyavka, T., & Baran, J. (2003). Pyridine-TiO₂ surface interaction as a probe for surface active centers analysis. *Appl. Surf. Sci.*, 214, 222-231.
- [3]. Blumstein, A. (1965). Polymerization of adsorbed monolayers: II. thermal degradation of the inserted polymers. *J. Polym. Sci.*, A 3, 2665-2673.
- [4]. Crosby, A. J., & Lee, J. Y. (2007). Polymer nanocomposites: the “nano” effect on mechanical properties. *Polym. Rev.*, 47, 217-229.
- [5]. Džunuzović, E., Vodnik, V., Jeremić, K., & Nedeljković J. M. (2009). Thermal properties of PS/TiO₂ nanocomposites obtained by in situ bulk radical polymerization of styrene. *Mater. Lett.*, 63, 908-810.
- [6]. Fischer, E. W., Sterzel, H. J., & Wegner, G. (1973). Investigation of the structure of solution grown crystals of lactide copolymers by means of chemical reactions. *Kolloid Z. Z. Polym.*, 251, 980-990.
- [7]. Fomin, V. A., & Guzeev, V. V. (2001). Biodegradable polymers, their present state and future aspects. *Prog. Rubb. Plastics Tech.*, 17, 186-204.
- [8]. Gnanasekaran, D., Madhavan, K., & Reddy, B. S. R. (2009). Developments of polyhedral oligomeric silsesquioxanes (POSS), POSS nanocomposites and their applications: a review. *J. Sci. Ind. Res.*, 68, 437-464.
- [9]. Gupta, A. P., & Kumar, V. (2007). New emerging trends in synthetic biodegradable polymers
 1. polylactide: a critique. *Eur. Polym. J.*, 43, 4053-4074.
- [10]. Haque, S., Rehman, I., & Darr, J. A. (2007). Synthesis and characterization of grafted nanohydroxyapatites using functionalized surface agents. *Langmuir*, 23, 6671-6676.

- [11]. Hojjati, B., Sui, R., & Charpentier, P. A. (2007) Synthesis of TiO₂/PAA nanocomposite by RAFT polymerization. *Polymer*, 48, 5850-5858.
- [12]. Li, Y., & Sun, X. S. (2010). Preparation and characterization of polymer–inorganic nanocomposites by in situ melt polycondensation of L-lactic acid and surface-hydroxylated MgO. *Biomacromolecules*, 11, 1847–1855.
- [13]. Paul, D. R., & Robeson, L. M. (2008). Polymer nanotechnology: nanocomposites. *Polymer*, 49, 3187-3204.
- [14]. Ray, S. S., & Bousmina, M. (2005). Biodegradable polymers and their layered silicate nanocomposites: in greening the 21st century materials world. *Prog. Mater. Sci.*, 50, 962-1079.
- [15]. Tsuji, H., Kawashima, Y., Takikawa, H., & Tanaka, S. (2007). Poly(l-lactide)/nano-structured carbon composites: conductivity, thermal properties, crystallization, and biodegradation. *Polymer*, 48, 4213-4225.
- [16]. Usuki, A., Kojima, Y., Kawasumi, M., Okada, A., Fukushima, Y., Kurauchi, T., & Kamigaito, O. (1993). Synthesis of nylon 6-clay hybrid. *J. Mater. Res.*, 8, 1179-1184.
- [17]. Hojjati, B., Sui, R., & Charpentier, P. A. (2007) Synthesis of TiO₂/PAA nanocomposite by RAFT polymerization. *Polymer*, 48, 5850-5858.
- [18]. Li, Y., & Sun, X. S. (2010). Preparation and characterization of polymer–inorganic nanocomposites by in situ melt polycondensation of L-lactic acid and surface-hydroxylated MgO. *Biomacromolecules*, 11, 1847–1855.
- [19]. Paul, D. R., & Robeson, L. M. (2008). Polymer nanotechnology: nanocomposites. *Polymer*, 49, 3187-3204.
- [20]. Ray, S. S., & Bousmina, M. (2005). Biodegradable polymers and their layered silicate nanocomposites: in greening the 21st century materials world. *Prog. Mater. Sci.*, 50, 962-1079.
- [21]. Tsuji, H., Kawashima, Y., Takikawa, H., & Tanaka, S. (2007). Poly(l-lactide)/nano-structured carbon composites: conductivity, thermal properties, crystallization, and biodegradation. *Polymer*, 48, 4213-4225.